The N-Terminal Transmembrane Domain of λ S Is Required for Holin but Not Antiholin Function[∇]

Rebecca White,[2]† Tram Anh T. Tran,[1]‡ Chelsey A. Dankenbring,[1]§ John Deaton,[1]¶ and Ry Young[1]*

Department of Biochemistry and Biophysics, Texas A&M University, 2128 TAMU, College Station, Texas 77843-2128,[1] and Department of Biology, Texas A&M University, College Station, Texas 77843-3528[2]

The λ *S* gene encodes a holin, S105, and an antiholin, S107, which differs by its Met-Lys N-terminal extension. The model for the lysis-defective character of S107 stipulates that the additional N-terminal basic residue keeps S107 from assuming the topology of S105, which is N-out, C-in, with three transmembrane domains (TMDs). Here we show that the N terminus of S105 retains its fMet residue but that the N terminus of S107 is fully deformylated. This supports the model that in S105, TMD1 inserts into the membrane very rapidly but that in S107, it is retained in the cytoplasm. Further, it reveals that, compared to S105, S107 has two extra positively charged moieties, Lys2 and the free N-terminal amino group, to hinder its penetration into an energized membrane. Moreover, an allele, $S105_{\Delta TMD1}$, with TMD1 deleted, was found to be defective in lysis, insensitive to membrane depolarization, and dominant to the wild-type allele, indicating that the lysis-defective, antiholin character of S107 is due to the absence of TMD1 from the bilayer rather than to its ectopic localization at the inner face of the cytoplasmic membrane. Finally, the antiholin function of the deletion protein was compromised by the substitution of early-lysis missense mutations in either the deletion protein or parental S105 but restored when both $S105_{\Delta TMD1}$ and holin carried the substitution.

In general, holins control the length of the infection cycle of double-stranded DNA phages (37). During late gene expression, the holin protein accumulates harmlessly in the bilayer until suddenly and spontaneously triggering the formation of holes in the membrane at an allele-specific time (13, 15). Holin genes are extremely diverse, but most can be grouped into two main classes based on the number of predicted transmembrane domains (TMDs): class I, with three TMDs and a predicted N-out, C-in topology, and class II, with two TMDs and a predicted N-in, C-in topology (38). Holin genes and function are subject to several levels of regulation, among which a particularly striking feature is the common occurrence of two potential translational starts, or dual-start motifs (5, 37), separated by only a few codons. Dual-start motifs are found in many holins of both of the two major classes; in nearly every case, the two starts are separated by at least one basic residue. The first dual-start motif to be characterized was that of λ *S*, the prototype class I holin gene (Fig. 1A and B). Translation initiation events occur at codons 1 and 3, giving rise to two products, S107 and S105, each named because of the length of its amino acid sequence; in the wild-type (wt) allele, two RNA structures define the ratio of initiations at the two start codons, resulting in an S105/S107 ratio of ~2:1.

Although they differ only by the Met-Lys N-terminal extension of S107, the two proteins have opposing functions; S105 is the holin and S107 the antiholin. The antiholin function is reflected by four principal features: first, when the Met3 start is inactivated, the mutant allele, designated *S107* (Fig. 1A), is lysis defective (26); second, the S107 protein binds and inhibits S105 specifically (3, 16); third, when S107 is produced in stoichiometric excess over S105, lysis is blocked for several times the length of the normal infection cycle (3, 4, 7, 16); and fourth, S107 antiholin function, i.e., inhibition of S105 hole formation, can be instantly subverted by collapsing the proton motive force, most easily done by addition of energy poisons to the medium (3). The predicted N-out, C-in topology and the requirement for the energized membrane led to a model in which S107 is initially inserted in the membrane with only two TMDs, with TMD1 being blocked from insertion by the presence of the positively charged residue, Lys2, whereas S105 has three TMDs (Fig. 1C) (39). From this perspective, S105-S107 complexes, which are approximately twice as numerous as the S105 homodimers, are defective in triggering hole formation. An appealing feature of this model is that when an S105-mediated hole formation event does occur in a cell, the resultant collapse of the membrane potential allows insertion of TMD1 of S107 into the membrane, instantly tripling the amount of active holin by making the previously inactive pool of S105-S107 complexes functional (38).

Some genetic and physiological evidence for the topology of the λ S proteins has been obtained using gene fusions. First, a fusion of the S gene at codon 105 with *lacZ* generates a functional, membrane-inserted β-galactosidase chimera, indicating, as expected, the cytoplasmic disposition of the highly

* Corresponding author. Mailing address: Department of Biochemistry and Biophysics, Texas A&M University, 2128 TAMU, College Station, TX 77843-2128. Phone: (979) 458-2070. Fax: (979) 458-2076. E-mail: ryland@tamu.edu.
† Present address: Sapphire Energy, Inc., 3115 Merryfield Row, San Diego, CA 92121.
‡ Present address: Department of Internal Medicine, Oncology Division, Simmons Comprehensive Cancer Center, University of Texas Southwestern Medical Center, 5323 Harry Hines Blvd., Dallas, TX 75390-9133.
§ Present address: Department of Biological Sciences, Purdue University, 915 W. State Street, West Lafayette, IN 47907-2054.
¶ Present address: Deerland Enzymes, 3800 Cobb International Blvd., Kennesaw, GA 30152.
∇ Published ahead of print on 6 November 2009.

FIG. 1. Gene, topology, and sequence of λ S. (A, top) The λ lysis cassette, including genes *S*, *R*, *Rz*, and *Rz1*, is shown, along with its promoter $p_{R'}$, and *Q*, encoding the late gene activator. The 5′ end of the class I holin gene *S* has two start codons, Met1, the start for S107, and Met3, the start for S105, and two RNA structures that regulate initiations at these codons. The *S105* and *S107* alleles have Leu (CUG) codons in place of the Met3 and Met1 codons, respectively. (B) Primary structure of S proteins. Missense changes relevant to the text are shown. Starts for S107 and S105 are indicated by asterisks. The three TMDs are boxed (13), and the extent of the Δ*TMD1* deletion is indicated. (C) Model for the membrane topology of S105, S107, and S105ₜₘD1. Topology and boundary residues for TMD1, -2, and -3 are based on Graschopf and Blasi (11) and Gründling et al. (13), respectively.

charged C terminus of the S protein (40). Second, Graschopf and Bläsi (12) demonstrated that S-mediated hole formation could be obtained with constructs where a secretory signal sequence was fused to the N termini of both S105 and S107. Lysis required the cleavage of the signal sequence by leader peptidase, and export of the signal-S107 form was slower than for the signal-S105 form. However, evidence for the topology of native forms of S has not been available. Moreover, no basis for the inhibitory character of S107 has been established. In the simplest view, the antiholin function could be due to the absence of TMD1 from the bilayer or the ectopic localization of TMD1 in the cytoplasm, or both. Here, we report studies directed at dissecting the precise role of topology in S107 function and correlating antiholin activity with its ability to heterodimerize with S105. The results are discussed in terms of a general model for the formation of the holin lesion and the role of dynamic membrane topology in its temporal regulation.

MATERIALS AND METHODS

Bacterial strains, bacteriophages, plasmids, culture growth, and phage titration. The strains and plasmids used in this work are described in Table 1. Media, growth conditions, and inductions of the λ lysis genes from a prophage and/or plasmids have been described previously (7, 13, 15, 30). Bacterial cultures were grown in standard LB medium supplemented with ampicillin (100 μg/ml) (LB-Ap), kanamycin (40 μg/ml) (LB-Km), and chloramphenicol (10 μg/ml) (LB-Cm), or some combination, when appropriate. The ability of *S* alleles to be triggered by membrane depolarization was assessed by adding dinitrophenol (DNP) to a final concentration of 5 mM. CHCl₃ was used at a 1% final concentration. *N*-Ethylmaleimide (NEM) and 1-10 phenanthroline were purchased from Sigma-Aldrich (St. Louis, MO). RY17456, which complements all lysis gene defects because it carries the lysis genes of phage 21 under the control of the λ late promoter, pR′, on plasmid pTP2 (Table 1), was used for determination of the efficiency of plating (EOP).

DNA manipulations, mutagenesis, and sequencing. Isolation of plasmid DNA, DNA amplification by PCR, DNA transformation, site-directed mutagenesis, and DNA sequencing were performed as previously described (13). Splicing by overlapping extension (SOE) PCR was performed as described previously (17). Oligonucleotides for PCR were obtained from Integrated DNA Technologies, Coralville, IA, and were used without further purification; sequences of the oligonucleotides used are available on request. Enzymes were purchased from

New England Biolabs, except for *Pfu* polymerase, which was from Stratagene. Automated fluorescence sequencing was performed at the Laboratory for Plant Genome Technology at Texas AgriLife.

Plasmid construction and generation of recombinant bacteriophage. The parental plasmid used was pS105 (Table 1), which is a medium-copy-number vector carrying the entire λ lysis cassette downstream of its native pR′ promoter (Fig. 1A). pS105 carries the *S105* allele, which produces the S105 holin but not the S107 antiholin. The plasmid pS105ₜₘD1 was constructed from pS105 by site-directed mutagenesis, with nucleotides (nt) 27 to 90 of the *S105* gene deleted. The plasmid pλ81 is identical to pS105 but has the lysis cassette from λ81, carrying the *R*am54 *R*am60 endolysin allele, cloned into the corresponding EcoRI and ClaI sites (λ nt 44972 to 46448), with a silent mutation (C to T at λ nt 44594) to ablate the second AatII site in the *R* gene. The EcoRV-ClaI fragment from pS105RzₐₘRz1ₐₘ containing a portion of the *R* gene and nonsense alleles of the *Rz Rz1* gene pair was cloned into pλ81, creating pλ81-2. The S105 gene from pS105 was then cloned into pλ81-2 via SOE PCR to create pS105RₐₘRzₐₘRz1ₐₘ, carrying the nonsense alleles of all the lysis genes except *S*. Ths plasmid was used to create pS107 RₐₘRzₐₘRz1ₐₘ, pS105ₐ₅₂ᵥ RₐₘRzₐₘRz1ₐₘ, pS105ₜₘD1RₐₘRzₐₘRz1ₐₘ, and pSₐₘRₐₘRzₐₘRz1ₐₘ by site-directed mutagenesis.

Lysis gene alleles were transferred to the phage context by recombination. For nonlytic alleles of *S105* (such as *S105ₜₘD1*), the cognate plasmids were transformed into RY17366 and individual transformants were grown up and induced as previously described (14). CHCl₃ was added to the cultures 2 h after induction. Lysates were cleared by centrifugation (3,000 rpm in a clinical centrifuge for 10 min) and used to reinfect early-log cultures of RY17341 at an input multiplicity of infection (MOI) of 5. Two hours after infection, CHCl₃ was added and the lysate again cleared. This enrichment step was repeated twice more, and the final lysate was used to lysogenize RY17303. For plaque-forming alleles, the method was the same except that the cleared lysates were directly plated on RY17341. Phage from purified plaques was used to lysogenize RY17303. Lysogens were selected by plating infected cells on LB-Cm plates at 30°C, screened by PCR for the presence of a single prophage as described by Powell et al. (25), and checked for the presence of *R*⁺ by cross-streaking with the hetero-immune *R*am phage λ84.

Purification of S proteins. His-tagged versions of S105, S107, and S105ₜₘD1 were purified as described previously (9), using the overexpression plasmids pET-S105₊₉₄, pET-S107₊₉₄, and pET-S105ₜₘD1, ₊₉₄. The last plasmid, encoding the His-tagged deletion protein, was constructed by site-directed mutagenesis of pET-S105₊₉₄. N-terminal sequencing of these proteins was performed at the Protein Chemistry Laboratory at the Texas Agricultural Experiment Station.

Purification of *Escherichia coli* deformylase. The plasmid pET-22B-def-CHT, encoding oligohistidine-tagged deformylase and kindly provided by Dehua Pei, was used to produce the deformylase in BL21(DE3) *slyD*::Tn*10*, as described

TABLE 1. Bacteriophages, strains, and plasmids used in this study

Phage, strain, or plasmid designation	Genotype and/or relevant features	Source or reference[a]
Phages		
λΔ(*SR*)	Δ(*stf-tfa*)::*cat c*I857 Δ(*SR*)	30
λ81	λ*c*I *R*am54 *R*am60; the *R*am54 and *R*am60 mutations, previously unsequenced, were found to be R_{Q26am} and R_{W73am}, respectively	Stock
λ84	λ*imm*^{434} *c*I R_{Q26am} R_{W73am}	Stock
λ*S105*	Δ(*stf-tfa*)::*cat c*I857 S_{M1L}	29
λ*S105*$_{A52V}$	Same as λ*S105*, but with an Ala52Val change in S105	
λ*S107*	Δ(*stf-tfa*)::*cat c*I857 S_{M3L}	
λ*S105*$_{ΔTMD1}$	Isogenic to λ*S105* except codons for TMD1 (nt 27–90, codons 9–30 of *S105* are deleted) (Fig. 1C)	
λ*Sam*	λS_{W56am} (also known as *S*am7)	
Strains		
MC4100	*E. coli* K-12 F⁻ *araD139* Δ(*argF-lac*)U169 *rpsL15 relA1 flbB3501 deo pstF25 rbsR*	Stock
BL21(DE3) *slyD*::Tn*10*	*E. coli* B hyper-expression strain (Novagen), converted to *slyD* mutant by P1 transduction	2
RY17303	MC4100Δ*tonA*	Stock
RY17366	MC4100Δ*tonA* [λΔ(*SR*)]	Stock
MG1655	F⁻ *ilvG rfb-50 rph-1*	Stock
RY16504	MG1655Δ*tonA lacI*�q Δ*lacY* pQ	
MDS12	MG1655 with 12 deletions, totaling 376,180 nt, including all cryptic prophages	20
RY17341	MDS12Δ*tonA*	
RY17456	MDS12Δ*tonA* pTP2	
Plasmids		
pQ	λ *Q* gene cloned into pZS*24; inducible with arabinose and IPTG (isopropyl-β-D-thiogalactopyranoside); Km^r	14
pS105	*S105 R Rz Rz1* genes of λ cloned into pBR322, Ap^r	15
pSwt	pS105 *S*⁺	16
pKB1	pS105 *S*am7	15
pS107	pS105 S_{M3L}	16
pS105$_{ΔTMD1}$	pS105 *S105*$_{ΔTMD1}$	
pS105$_{ΔTMD1,A52G}$	pS105 *S105*$_{ΔTMD1,A52G}$	
pλ81	pS105 *S*⁺ R_{Q26am} R_{W73am}	
pλ81-2	pS105 *S*⁺ R_{Q26am} R_{W73am} Rz_{Q100am} Rz_{W38am}	
pS105$_{ΔTMD1,A52V}$	pS105 *S105*$_{ΔTMD1,A52V}$	
pS105R$_{am}$Rz$_{am}$Rz1$_{am}$	pS105 R_{Q26am} R_{W73am} Rz_{Q100am} Rz_{W38am}, plus a unique KpnI site constructed in *R*	
pS105Rz$_{am}$Rz1$_{am}$	pS105 R_{Q26am} R_{W73am} Rz_{Q100am} Rz_{W38am}	
pS107R$_{am}$Rz$_{am}$Rz1$_{am}$	pS107 R_{Q26am} R_{W73am} Rz_{Q100am} Rz_{W38am}	
pS105$_{ΔTMD1}$R$_{am}$Rz$_{am}$Rz1$_{am}$	pS105$_{ΔTMD1}$ R_{Q26am} R_{W73am} Rz_{Q100am} Rz_{W38am}	
pS105$_{A52V}$R$_{am}$Rz$_{am}$Rz1$_{am}$	pS105 *S105*$_{A52V}$ R_{Q26am} R_{W73am} Rz_{Q100am} Rz_{W38am}	
pS$_{am}$R$_{am}$Rz$_{am}$Rz1$_{am}$	pS105S_{W56am} R_{Q26am} R_{W73am} Rz_{Q100am} Rz_{W38am}	
pTP2	Isogenic to pS105, but with the lysis genes S^{21}, R^{21}, Rz^{21}, and $Rz1^{21}$ of lambdoid phage 21; the presence of this plasmid in an indicator strain complements defects in all λ lysis genes for plaque formation.	See supporting information, Table 1 of Park et al. (24)
pET-S105$_{τ94}$	pETlla *S105*$_{τ94}$; product has GGH6GG oligohistidine tag inserted between residues 94 and 95	30
pET-S107$_{τ94}$	Isogenic to pET-S105$_{τ94}$ except in *S107*$_{τ94}$	
pET-S105$_{ΔTMD1τ94}$	Isogenic to pET-S105$_{τ94}$ except in *S105*$_{ΔTMD1}$	
pET-22B-def-CHT	pET22B (Novagen), encoding oligohistidine-tagged *E. coli* deformylase	27

[a] Unless otherwise indicated, strains, phages, and plasmids were constructed in this study. Stock, laboratory stock.

previously (27). The enzyme was purified by immobilized metal affinity chromatography to a final concentration of 5 mg/ml. The activity of the purified enzyme was determined using the tri-peptide formyl-Met-Ala-Ser (Sigma) as the substrate. The appearance of N-terminal amines was monitored using 2,4,6-trinitrobenzenesulfonic acid (10).

Deformylation of S105. To remove the formyl group on S105, 50 μl of purified S105 (50 μg) was added to 110 μl of 0.1 M MOPS (morpholinepropanesulfonic acid), 0.25 M KCl (pH 7.2), 5 μl catalase (10 mg/ml in water; Sigma), and 5 μl of purified deformylase at 5 mg/ml. The reaction mixture was incubated at 30°C for 20 m, and the reaction was stopped by trichloroacetic acid (TCA) precipitation. The protein pellet was resuspended in 40 μl of 1% Empigen BB (Calbiochem, La Jolla, CA), 20 mM BES [*N,N*-bis(2-hydroxyethyl)-2-aminoethanesulfonic acid], 0.1 M NaCl, pH 7. After addition of 20 μl of 2× sodium dodecyl sulfate-polyacrylamide gel electrophoresis (SDS-PAGE) sample loading buffer, the samples were boiled for 5 min and subjected to 16% SDS-PAGE. The S105 band was excised and used for N-terminal sequencing by the Protein Chemistry Laboratory at Texas A&M University.

Protein analysis. For TCA precipitations, 1-ml culture aliquots were added to 111 μl of cold, 6.1 N trichloroacetic acid and then placed on ice for 30 min. The precipitate was collected by centrifugation (18,000 × *g* in a tabletop microcentrifuge for 30 min) and washed once with acetone, with complete resuspension of the pellet. Pellets were air dried, resuspended in sample loading buffer, and then analyzed by SDS-PAGE as previously described (14), except that the gels used for Fig. 7 were not precast. Western blotting with anti-S antibodies (13) and oxidative disulfide bridge formation by Cu-phenanthroline treatment of membranes (16) were carried out as previously described. Relative band intensities were determined by analysis using ImageJ (http://rsb.info.nih.gov/ij/docs/intro.html).

TABLE 2. Sequencing of purified S proteins

Sample[a]	Repetitive yield (%)	Sequence(s)
S105	0	
S107*	82	MKLPEK
Def-treated S105	>95	XXHDLLA, XXXHDLLA[b]
S105$_{\Delta TMD1}$	91	PEKHD

[a] Purified His-tagged proteins. S107* is the product of the $S107_{\tau94}$ allele, in which codon 3, the start codon of the *S105* reading frame, is converted to a CTG (Leu) (30).

[b] Two overlapping sequences amounting to >95% of the total repetitive yield were obtained. This is likely due to contaminating activity of methionine-aminopeptidase, as previously reported (21, 32).

Phage accumulation after the induction of λ lysogens. At various times after induction, 1-ml aliquots were treated with 1% CHCl$_3$ to release progeny phage and the titer was determined by plating on lawns of RY17456. Plaques from triplicate platings were counted after 12 to 16 h of incubation at 37°C, and the averages from two experiments were used.

Viability assays. Two-milliliter samples of induced cultures of RY16504 carrying plasmids with the *S105* allele indicated in Fig. 2 and nonsense alleles of the other three lysis genes were placed on ice. Half of each sample was serially diluted on ice and plated in triplicate on LB-Km-Ap, and the remainder was precipitated with TCA, as previously described (33), and analyzed by immunoblotting. Colonies from three separate experiments were counted after 12 to 16 h of incubation at 37°C.

Chemical mutagenesis of phage. Hydroxylamine mutagenesis of λ$S105_{\Delta TMD1}$ phage was performed as described previously (8). Following mutagenesis, the titers of the samples were determined by plating on lawns of the complementing indicator, RY17456. PFU (10^8) were plated at an MOI of ~0.1 to 0.2 on RY17341 on each of 10 to 15 plates. No plaques were observed in three experiments, with a total of ~5 × 10^9 virions plated. Ethylmethane sulfonate (EMS) mutagenesis of λ$S105_{\Delta TMD1}$ was performed as described previously (22), with the following adaptations. A logarithmic culture of RY17434 was induced at an A_{550} of ~0.2, and EMS was added after 15 min. The culture was grown for 4 h at 37°C, harvested by centrifugation, washed in λ dilution buffer, resuspended in 2 ml of λ dilution buffer, and disrupted in a French pressure cell (Spectronic Instruments, Rochester, NY) at 16,000 lb/in^2 (1 lb/in^2 = 6.89 kPa). The titer of the lysate was determined on lawns of RY17456. A control culture of RY17341 was treated identically, except that instead of being passed through a French pressure cell, the culture was serially diluted and plated on LB plates and LB plates containing 100 μg/ml rifampin to measure survival and mutation frequency. An aliquot containing 10^8 PFU was plated at an MOI of ~0.1 to 0.2 on RY17341 on each of 12 plates. The experiment was repeated twice, and no plaques were observed.

RESULTS

The N terminus of S105, but not S107, retains its fMet residue. Membrane proteins that achieve N-out topology without a cleavable signal sequence are relatively uncommon, but one example, Lep, or signal peptidase II, has been studied in detail. The N terminus of Lep was found to retain its N-terminal formyl group, as a consequence of its rapid externalization to the periplasm, thereby avoiding the normal processing by cytoplasmic polypeptide deformylase, Def (35). If the model indicating that S105 and S107 have different topologies is correct, the N terminus of S105, but not S107, might also escape deformylation. To test this idea, the S105 and S107 proteins were purified and subjected to N-terminal sequencing. The N-terminal sequence for S107 was found to correspond exactly to that predicted from the dual-start motif and was obtained at a high repetitive yield (Table 2). In contrast, no sequence information was obtained for S105, suggesting that its α-amino group was blocked. When S105 was pretreated with purified *E. coli* Def, a sequence consistent with transla-

tional initiation at the Met3 codon was obtained (Table 2), demonstrating that S105 indeed retains the N-terminal fMet residue. This directly supports the model for S105 and S107 topology and suggests that the N terminus of S105 exits the cytoplasm rapidly enough to escape cytoplasmic deformylation. Moreover, this suggests that the inability of S107 to assume an S105-like topology in the energized inner membrane is due to two extra positive charges in the protonated free amino groups at Lys2 and the N terminus, compared to none in S105.

TMD1 of S is essential for holin activity. In view of the topological difference between S105 and S107, it was of interest to know whether TMD1 is required for the holin function of S105, the antiholin function of S107, or both. To address these questions, we deleted codons 9 to 30, which encode TMD1, from *S105* to make the allele $S105_{\Delta TMD1}$. We also constructed the $S105_{\Delta TMD1}$ equivalents of $S105_{A52G}$ and $S105_{A52V}$, which are, respectively, early-lysis and lysis-defective alleles of S105 (14, 18). $S105_{\Delta TMD1}$ proved to be nonlytic in the context of the phage and also nonlethal when induced from a plasmid (Fig. 2A and B). After 1 h of induction, the plasmid-borne deletion allele had no effect on host viability and was indistinguishable from a null S_{W56am} allele, the lysis-defective $S105_{A52V}$ allele, and the *S107* allele, which produces only the S107 antiholin. Moreover, after prolonged incubation, the deletion allele, like the null allele S_{W56am}, retained its nonlethal character, whereas a significant proportion of cells expressing *S107* were killed (Fig. 2B, last four bars), presumably reflecting the eventual penetration of the membrane by the N-terminal domain of S107. When the deletion allele was recombined onto the phage, not only was there an absolute lysis defect, but progeny accumulated for hours after induction, indicating a complete absence of membrane toxicity (Fig. 2C). These phenotypic defects were not due to the mislocalization or instability of the $S105_{\Delta TMD1}$ protein, which accumulated exclusively in the membrane (data not shown) and to higher levels than either S105 or S107 (Fig. 3A). The higher expression is consistent with the loss, in the deletion of codons 9 to 30 in $S_{\Delta TMD1}$, of a regulatory RNA secondary structure spanning codons 11 through 16 (Fig. 1A), previously shown to be required for regulation of the S105 reading frame (4, 23, 26). Moreover, N-terminal sequencing of purified $S105_{\Delta TMD1}$ protein revealed that its N terminus was unblocked, indicating that it was retained in the cytoplasm (Table 2). Thus, deletion of TMD1 did not affect the topology of the remainder of the protein.

When plated on wt *E. coli* K-12 lawns, λS105$_{\Delta TMD1}$ generated plaques but at a much lower frequency (efficiency of plating [EOP], ~1.5 × 10^{-8}) than λS$_{W56am}$, which plates with an EOP of ~2 × 10^{-5} under these conditions. However, the plaques derived from λS105$_{\Delta TMD1}$ proved to be pseudorevertants derived from recombination with cryptic prophage elements, resulting in replacement of the S105$_{\Delta TMD1}$ gene with that of a heterologous functional holin (data not shown; also see Kaiser [19]). On strain MDS12, from which all the vestigial prophage elements of the *E. coli* chromosome have been deleted (20), no plaque-forming phage could be isolated, even with extensive chemical mutagenesis, from more than 5 × 10^9 virions (not shown; see Materials and Methods). The much higher reversion rate of λS$_{W56am}$ under the same conditions
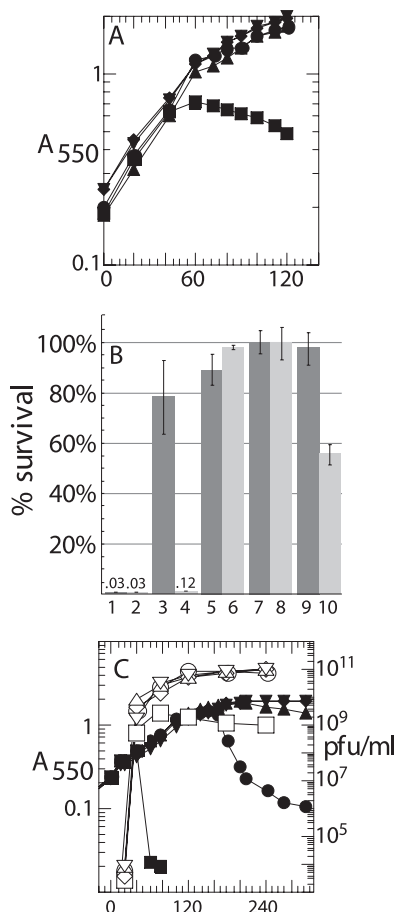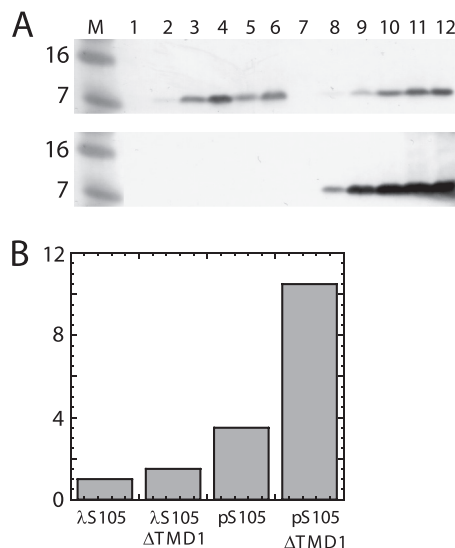
FIG. 3. Accumulation of *S* gene products after induction. (A) RY17303 cultures carrying λ*S105* (lanes 1 to 6, upper blot), λ*S107* (lanes 7 to 12, upper blot), λ*S*am (lanes 1 to 6, lower blot), or λ*S105*$_{\Delta TMD1}$ (lanes 7 to 12, lower blot) were induced and samples taken by TCA precipitation at 0, 15, 30, 45, 60, and 90 min after induction (respectively for each grouping of lanes 1 to 6 and 7 to 12), resolved by 16% Tris-Tricine SDS-PAGE, and analyzed by Western blot analysis using anti-S antibodies. The λ*S105* sampling was curtailed after culture lysis. Lane M, molecular weight markers (in thousands). (B) Quantification of S105 and S105$_{\Delta TMD1}$. Experiments were performed as described for panel A, except RY17303 carried the indicated prophage or plasmid, samples were taken at 15 min after induction, and band intensities (*y* axis) were quantified, relative to the amount in the λ*S105* sample.

FIG. 2. S105$_{\Delta TMD1}$ is an absolute defective holin. (A and C) Cultures of the nonsuppressing hosts RY16504 (*lacI*^{q}) (A) and RY17303 (Δ*lac*) (C) carrying the indicated prophages and/or plasmids were induced at time zero and monitored for A_{550} (filled symbols) as described in Materials and Methods. The abscissa is time after induction (min) for all panels except B. (A) Plasmids pS105R$_{am}$Rz$_{am}$Rz1$_{am}$ (■), pS107R$_{am}$Rz$_{am}$Rz1$_{am}$ (●), pS105$_{A52V}$R$_{am}$Rz$_{am}$Rz1$_{am}$ (▲), pS105$_{\Delta TMD1}$R$_{am}$Rz$_{am}$Rz1$_{am}$ (◆), and pS105$_{am}$R$_{am}$Rz$_{am}$Rz1$_{am}$ (▼). (B) Titers of surviving phage in cultures from panel A, plated at 60 min (odd-numbered bars) or 120 min (even-numbered bars). *S* alleles *S105* (bars 1 and 2), *S107* (bars 3 and 4), S_{A52V} (bars 5 and 6), *S105*$_{W56am}$ (bars 7 and 8), and *S105*$_{\Delta TMD1}$ (bars 9 and 10). Numbers above bars 1, 2, and 4 indicate percent survival. (C) Prophages λS105 (■), λS107 (●), λS105$_{A52V}$ (▲), λS105$_\Delta$TMD1$_\Delta$ (◆), and λS105$_{W56am}$ (▼). Accumulations of phage (PFU) are also shown with corresponding open symbols.

suggests that the deletion allele cannot be converted to lytic function even with several mutations, despite its intrinsically higher expression level. We conclude that the N-terminal TMD of S105 is essential for its holin function, although not for its localization or synthesis.

The antiholin character of S107 is due to the absence of TMD1 from the bilayer. The antiholin character of S107 could be due to the lack of TMD1 in the bilayer or the presence of the ectopically localized TMD1 in the cytoplasm, or both. To address this issue, we next decided to test the S105$_{\Delta TMD1}$ protein for antiholin function. Accordingly, either the S105$_{\Delta TMD1}$ or the S107 allele in its normal transcriptional context was introduced on a medium-copy-number plasmid into a lysogen carrying the λS105 prophage. Lysogenic induc-

tion of these strains results in transactivation of the plasmid genes, concomitant with the onset of late gene expression in the prophage. The presence of pS107 or pS105$_{\Delta TMD1}$ in *trans* resulted in identical levels of inhibition of lysis (Fig. 4). Thus, the *S105*$_{\Delta TMD1}$ allele is dominant negative and its product can function as an antiholin. Unlike S107 and consistent with the observation that TMD1 is essential for holin function, S105$_{\Delta TMD1}$ could not be triggered by the addition of energy poisons (Fig. 4A, open circles). Moreover, unlike with S107, which is sensitive to energy poisons (Fig. 4B), the ability of S105$_{\Delta TMD1}$ to inhibit the function of S105 could not be subverted by addition of DNP (Fig. 4A, open squares and triangles). These results suggest that S107 antiholin function is determined by the lack of TMD1 in the membrane, and its leakiness and its ability to be triggered by energy poisons reflect the imperfect barrier of the bilayer for transit of TMD1.

The *S105*$_{\Delta TMD1}$-mediated block was also reflected in the inability of λS105 to plate (EOP, $\sim 10^{-2}$) on lawns carrying the plasmid pS105$_{\Delta TMD1}$, although it plated near normal efficiency (EOP, ~ 0.6) on lawns carrying pS107 (Fig. 5). Presumably, this reflects the eventual collapse of the proton motive force in the infected cells, which, with S107 but not S105$_{\Delta TMD1}$, allows penetration of TMD1 into the bilayer and thus conversion to the functional holin form. Even if this occurred very late in each infection cycle, the ability to form plaques would be buffered by the greatly increased burst size (26). Part of the stricter barrier to plaque formation in cells carrying the plas-
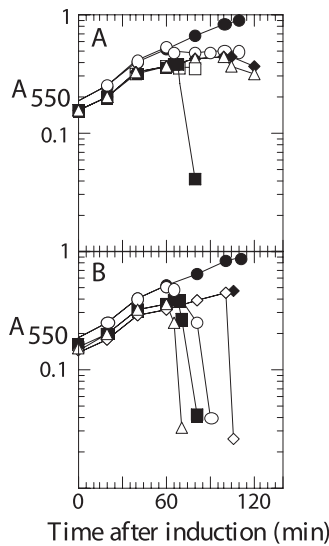
FIG. 4. S105$_{\Delta TMD1}$ is an untriggerable antiholin. Cultures carrying the indicated prophage, with or without the indicated transactivation plasmid, were induced and monitored as described for Fig. 2. (A) Inductions with or without pS105$_{\Delta TMD1}$R$_{am}$Rz$_{am}$Rz1$_{am}$ in *trans* were carried out with λ*S105* (■), λ*S105*$_{\Delta TMD1}$ (●), λ*S105*$_{\Delta TMD1}$ with DNP added at 40 min (○), λ*S105* plus pS105ΔTMD1 (◆), λ*S105* plus pS105$_{\Delta TMD1}$R$_{am}$Rz$_{am}$Rz1$_{am}$ with DNP added at 40 min (□), and λ*S105* plus pS105$_{\Delta TMD1}$R$_{am}$Rz$_{am}$Rz1$_{am}$ with DNP added at 80 min (△). (B) Inductions with or without pS107R$_{am}$Rz$_{am}$Rz1$_{am}$ in *trans* were carried out with λ*S105* (■), λ*S107* (●), λ*S107* with DNP added at 40 min (○), λ*S105* plus pS107R$_{am}$Rz$_{am}$Rz1$_{am}$ (◆), λ*S105* plus pS107R$_{am}$Rz$_{am}$Rz1$_{am}$ with DNP added at 40 min (△), and λ*S105* plus pS107R$_{am}$Rz$_{am}$Rz1$_{am}$ with DNP added at 80 min (◇).

mid-borne S105$_{\Delta TMD1}$ allele may be due to increased production of the deletion product, relative to the level of S105 produced by the infecting phage. Indeed, quantitative Western blotting revealed that the amount of S105$_{\Delta TMD1}$ produced from the transactivation plasmid construct was about 7-fold higher than the amount of S105 produced from the phage context (Fig. 3B). When the deletion allele was transferred to the context of the phage and *S105* to the plasmid, spontaneous
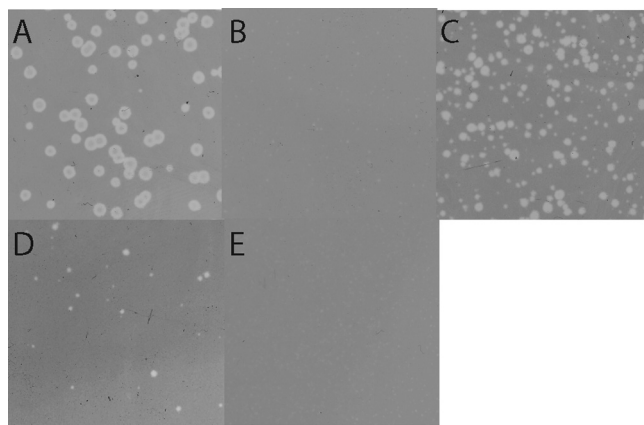
FIG. 5. Allele-specific inhibition of plaque formation in lawns carrying *S105*$_{\Delta TMD1}$. Dilutions of λ*S105* were plated on lawns of RY17341 carrying transactivating plasmids with the indicated *S* allele. (A) *S$_{W56am}$*; (B) *S105*$_{\Delta TMD1}$; (C) *S107*; (D) *S105*$_{\Delta TMD1,A52G}$; (E) *S105*$_{\Delta TMD1,A52V}$.
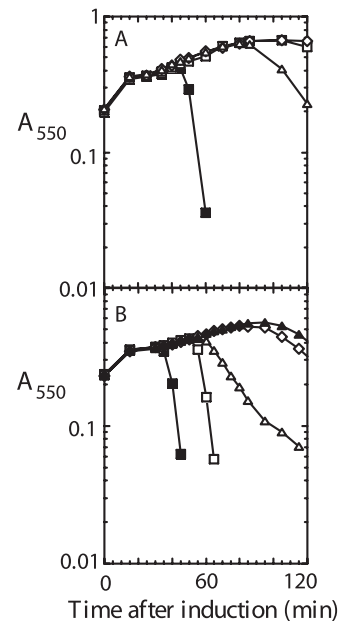
FIG. 6. Allele-specific inhibition of λ*S105* lysis by *S105*$_{\Delta TMD1}$. RY17303 cultures bearing the indicated prophage and carrying the transactivation plasmid with the indicated allele were induced and monitored as described for Fig. 2. (A) All cultures had λ*S105* with the plasmid allele *S$_{W56am}$* (■), *S105*$_{\Delta TMD1}$ (□), *S105*$_{\Delta TMD1,A52V}$ (◇), or *S105*$_{\Delta TMD1,A52G}$ (△). (B) ■, λ*S105*$_{A52G}$ with *S$_{W56am}$*; □, λ*S105* with *S$_{W56am}$*; △, λ*S105*$_{A52G}$ with *S105*$_{\Delta TMD1}$; ▲, λ*S105* with *S105*$_{\Delta TMD1}$; ◇, λ*S105*$_{A52G}$ with *S105*$_{\Delta TMD1,A52G}$.

lysis was observed (Fig. 6A), but the lengthy delay of the triggering time (from 30 min with pS105 alone to ~65 min for pS105 in *trans* to the S105$_{\Delta TMD1}$ prophage) indicates the antiholin character of *S105*$_{\Delta TMD1}$. These results indicate that S107 antiholin function derives from the absence of TMD1 in the membrane rather than from its ectopic localization in the cytoplasm.

The dependence of holin and antiholin function on TMD2-TMD2 interactions. Previous studies have indicated that the S107 antiholin inhibits S105 by a homotypic TMD2-TMD2 interaction, detected by the formation of disulfides between Cys51 residues as a result of treating membrane fractions with Cu^{2+}-phenanthroline (Cu-Phe). This is also the case for the deletion allele (Fig. 7). For the inductions with the *S105* allele on the prophage and the deletion allele on the plasmid that do not ultimately result in lysis, S105-S105$_{\Delta TMD1}$ heterodimers and S105$_{\Delta TMD1}$ homodimers could be detected, but no S105 homodimers could (Fig. 7A, lane 7, and B, lanes 2 and 3). In contrast, S105 homodimers could be detected in inductions which do result in lysis: with *S105* alone, in either the plasmid or phage context, and with *S105* on the plasmid and the deletion allele on the prophage (Fig. 7A and B). Interestingly, two mutations in TMD2 that cause a lack of plaque-forming ability, A52V and A52G, have opposite effects on the antiholin character of the deletion protein. A52G, which causes catastrophically early lysis at or near the end of the eclipse period in the context of *S105* (18), decreases the ability of S105$_{\Delta TMD1}$ to inhibit S105, as reflected in lysis profiles (Fig. 6A) and in plating ability (Fig. 5D), suggesting a weakened TMD2-TMD2 interaction because of the Ala-Gly mismatch at position 52
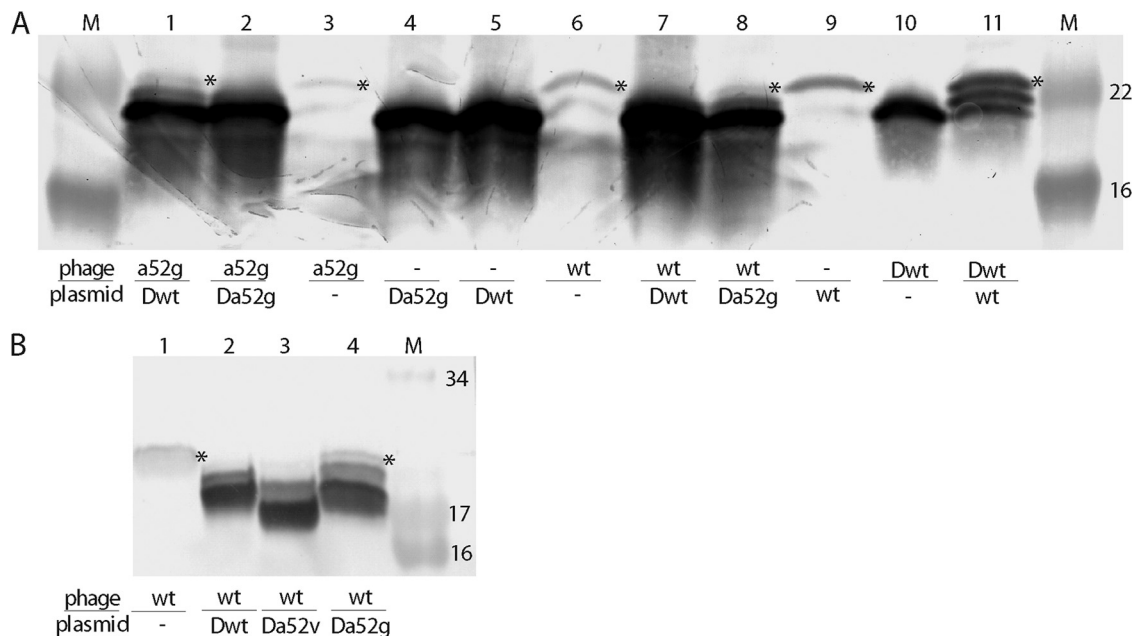
FIG. 7. Allele-specific inhibition by S105$_{\Delta TMD1}$ correlates with S105 homodimer formation. Membranes prepared from inductions with the indicated prophage and/or transactivation plasmid were treated with Cu-phenanthroline, resolved by SDS-PAGE, and analyzed by Western blotting. An asterisk to the right of a band indicates the position of the disulfide-linked S105 homodimer. Below the panels, the *S* alleles on the phages and plasmids are indicated by the following abbreviations: wt, *S105*; a52g, *S105$_{A52G}$*; Δ, ΔTMD1; Δwt, *S105$_{\Delta TMD1}$*; Δa52g, *S105$_{\Delta TMD1,A52G}$*. M, molecular mass markers, with approximate masses (in thousands) indicated to right of the blot in each panel. (A) Results of 12 to 20% Tris-glycine SDS-PAGE. Lanes: 1, λ*S105$_{A52G}$*, plasmid *S105$_{\Delta TMD1}$*; 2, λ*S105$_{A52G}$*, plasmid *S105$_{\Delta TMD1,A52G}$*; 3, λ*S105$_{A52G}$*; 4, plasmid *S105$_{\Delta TMD1,A52G}$*; 5, plasmid *S105$_{\Delta TMD1}$*; 6, λ*S105*; 7, λ*S105*, plasmid *S105$_{\Delta TMD}$*; 8, λ*S105*, plasmid *S105$_{\Delta TMD,A52G}$*; 9, plasmid *S105*; 10, λ*S105$_{\Delta TMD1}$*; 11, λ*S105$_{\Delta TMD1}$*, plasmid *S105*. (B) Results of 16% Tris-Tricine SDS-PAGE. Lanes: 1, λ*S105*; 2, λ*S105*, plasmid *S105$_{\Delta TMD1}$*; 3, λ*S105*, plasmid *S105$_{\Delta TMD1,A52V}$*; 4, plasmid *S105$_{\Delta TMD1,A52G}$*.

between the altered deletion protein and wt S105. In contrast, A52V, which blocks plaque formation in the context of *S105* because it is an absolute lysis-defective mutation, has no effect on the antiholin character of S105$_{\Delta TMD1}$ (Fig. 5E and 6A). In this case, the TMD2-TMD2 interaction is apparently unimpaired. Further, for A52G, this defect in inhibition could be suppressed by the same change in S105 (Fig. 6B), suggesting that resolving the mismatch restored the TMD2-TMD2 interaction. Moreover, restoration of inhibition was correlated with the absence of holin homodimers after Cu-Phe treatment (Fig. 7A, lane 2).

DISCUSSION

The dual-start motif is one of the most notable features of holin genes and serves to highlight the importance of the regulation of lysis timing, since the two translational start codons give rise to two polypeptides that, despite near identity in sequence, have opposing functions as the holin and antiholin. Here, we provide biochemical evidence for the difference in topology, present data that define the role of that difference in regulating hole formation, and describe experiments that relate antiholin function to homotypic TMD2-TMD2 interactions.

The N terminus of TMD1 is periplasmic. S105 has three TMDs with N-out and C-in (Fig. 1B and C). Here we show that the native S105 protein retains the formyl moiety on its N terminus but that S107 is quantitatively deformylated. Leader

peptidase, another N-out integral membrane protein with multiple TMDs, has also been shown to retain its N-formyl group. This finding supports the difference in topology between S105 and S107 and indicates that TMD1 of S105 enters the bilayer so rapidly after synthesis that it avoids processing by deformylase. It should be noted that the single positive charge of the Lys2 residue need only retard the entry of the N terminus of S107 into the membrane long enough for Def-mediated deformylation, which leaves S107 with two positive charges at its N terminus and thus presumably even more refractory to export against the polarity of the energized membrane. *S* alleles modified to have three or more basic residues after codon 1 are defective and not able to be triggered by energy poisons (31), suggesting that there is a limit to the ability to impose potential-dependent dynamic character on TMD1. A finely tuned balance between the retention and export of the N-terminal TMD is also reflected in the properties of the S^{21}68-S^{21}71 holin-antiholin pair encoded by the pinholin gene, *S^{21}* (24). Although the topological change is different, in that TMD1 escapes from the membrane rather than entering it, it is still required for hole formation. However, the single charge confers on the longer form a somewhat more subtle delay of about 20 min in the topological change. To obtain an antiholin form that cannot be triggered, it was necessary to append an oligopeptide sequence containing two positive charges to the N terminus of the shorter form. The more drastic effect of the second charge in this case may reflect the more difficult ener-

getics of removing a TMD from the bilayer rather than inserting it.

The antiholin character of S107 is due to the absence of TMD1 from the bilayer. The relationship of the functional and topological differences between S105 and S107 has previously not been addressed. That is, the antiholin character of S107 could be due to the presence of the ectopically located TMD1 or to the absence of TMD1 from the bilayer, or both. Here we show that S105$_{\Delta TMD1}$ has the same antiholin character as S107, strongly indicating that it is the absence of TMD1 from the membrane that underlies antiholin function. Moreover, the antiholin effects of the deletion protein are more stable in vivo and cannot be subverted by collapsing the membrane potential, further supporting the notion that it is the membrane penetration of TMD1 that defines the ability of uncouplers and energy poisons to collapse antiholin inhibition. The absolute-lysis-defective character of the deletion protein also suggests that TMD1 is required for hole formation.

Similar antiholin properties have been reported for a truncation of the class I holin, Hol, of the *Listeria* phage A118 (36). Clones of *hol* with a deletion of the 13 N-terminal codons of the 96-codon reading frame were shown to be nonfunctional when they were substituted for the *S* gene in a λ chimera. However, no evidence for the topological disposition of TMD1 in the parental or deletion allele was obtained, which is problematic because the deletion still leaves a potential 19-amino-acid N-terminal TMD. Moreover, expression of this A118 *hol* deletion allele from the same plasmid-borne λ pR′ context used here in the experiments with *S* and *S*$_{\Delta TMD1}$ was lethal to the host. Finally, the limitations of *Listeria* phage genetics did not allow rigorous determination of whether or not the shorter protein was produced from either the parental or deletion allele in *Listeria*.

The results presented here indicate that the antiholin character of S105$_{\Delta TMD1}$ derives from the loss of TMD1, which eliminates hole-forming activity while retaining the ability to bind specifically to S105. The requirement for TMD1 is not surprising, since missense changes in TMD1 abrogate hole formation without affecting accumulation (26). However, it should be noted that it is not necessary for an antiholin to have TMD-TMD interactions to block hole formation; in phage T4, the antiholin, gp*rI*, is a soluble periplasmic protein when it binds to the periplasmic domain of the holin, gp*t* (34).

Protein-protein interactions in the timing of lysis. Antiholin inhibition is not the central modality by which holin function is temporally regulated. With the phage λ, 21, and T4 systems, representing class I, II, and III holins, it has been shown that elimination of the antiholin leaves the intrinsic timing function intact. Antiholin function provides fine-tuning of the timing, in the cases of λ (3, 26) and phage 21 (1, 6), or a mechanism for environmental signals for overriding the intrinsic timing, in the case of T4 (28). The key feature of holin function is saltatory triggering of hole formation at a time built in to the primary structure. Moreover, single missense changes can confer drastic differences on the triggering time, best illustrated by opposing phenotypes of the early-lysis *S105*$_{A52G}$ and nonlytic *S105*$_{A52V}$ alleles. Here we have presented results suggesting that an Ala-Gly mismatch at position 52 impairs the homotypic TMD2-TMD2 interaction involved in dimerization and that resolution of the mismatch, i.e., to the mutant Gly-Gly or to

the wt Ala-Ala, restores this interaction. Similar phenotypic "mismatch" sensitivity was observed when the original library of lysis-defective *S* mutants was tested for their dominant/recessive character (26). A number of these lysis-defective mutants exhibited an unexpected form of dominance, in that they accelerated lysis timing in the presence of the wt allele. Since *S* encodes both the holin and antiholin, the existence of the "antidominant" alleles was most easily explained by invoking differential effects on holin and antiholin forms. The results presented here suggest instead that intimate helical packing of TMD2 defines the dimerization step that is required for both the hole formation pathway and antiholin function.

REFERENCES

1. **Barenboim, M., C. Y. Chang, F. dib Hajj, and R. Young.** 1999. Characterization of the dual start motif of a class II holin gene. Mol. Microbiol. **32:**715–727.
2. **Bernhardt, T. G., I. N. Wang, D. K. Struck, and R. Young.** 2001. A protein antibiotic in the phage Qβ virion: diversity in lysis targets. Science **292:**2326–2329.
3. **Bläsi, U., C. Y. Chang, M. T. Zagotta, K. Nam, and R. Young.** 1990. The lethal λ *S* gene encodes its own inhibitor. EMBO J. **9:**981–989.
4. **Bläsi, U., K. Nam, D. Hartz, L. Gold, and R. Young.** 1989. Dual translational initiation sites control function of the λ *S* gene. EMBO J. **8:**3501–3510.
5. **Bläsi, U., and R. Young.** 1996. Two beginnings for a single purpose: the dual-start holins in the regulation of phage lysis. Mol. Microbiol. **21:**675–682.
6. **Bonovich, M. T., and R. Young.** 1991. Dual start motif in two lambdoid S genes unrelated to lambda S. J. Bacteriol. **173:**2897–2905.
7. **Chang, C. Y., K. Nam, and R. Young.** 1995. *S* gene expression and the timing of lysis by bacteriophage λ. J. Bacteriol. **177:**3283–3294.
8. **Davis, R. W., D. Botstein, and J. R. Roth.** 1980. Advanced bacterial genetics. Cold Spring Harbor Laboratory, Cold Spring Harbor, NY.
9. **Deaton, J., C. G. Savva, J. Sun, A. Holzenburg, J. Berry, and R. Young.** 2004. Solubilization and delivery by GroEL of megadalton complexes of the lambda holin. Protein Sci. **13:**1778–1786.
10. **Fields, R.** 1972. The rapid determination of amino groups with TNBS. Methods Enzymol. **25:**464–468.
11. **Graschopf, A., and U. Bläsi.** 1999. Functional assembly of the lambda S holin requires periplasmic localization of its N-terminus. Arch. Microbiol. **172:**31–39.
12. **Graschopf, A., and U. Bläsi.** 1999. Molecular function of the dual-start motif in the λ *S* holin. Mol. Microbiol. **33:**569–582.
13. **Gründling, A., U. Bläsi, and R. Young.** 2000. Biochemical and genetic evidence for three transmembrane domains in the class I holin, λ S. J. Biol. Chem. **275:**769–776.
14. **Gründling, A., U. Bläsi, and R. Young.** 2000. Genetic and biochemical analysis of dimer and oligomer interactions of the λ *S* holin. J. Bacteriol. **182:**6082–6090.
15. **Gründling, A., M. D. Manson, and R. Young.** 2001. Holins kill without warning. Proc. Natl. Acad. Sci. U. S. A. **98:**9348–9352.
16. **Gründling, A., D. L. Smith, U. Bläsi, and R. Young.** 2000. Dimerization between the holin and holin inhibitor of phage lambda. J. Bacteriol. **182:**6075–6081.
17. **Ho, S. N., H. D. Hunt, R. M. Horton, J. K. Pullen, and L. R. Pease.** 1989. Site-directed mutagenesis by overlap extension using the polymerase chain reaction. Gene **77:**51–59.
18. **Johnson-Boaz, R., C. Y. Chang, and R. Young.** 1994. A dominant mutation in the bacteriophage lambda *S* gene causes premature lysis and an absolute defective plating phenotype. Mol. Microbiol. **13:**495–504.
19. **Kaiser, K.** 1980. The origin of Q-independent derivatives of phage lambda. Mol. Gen. Genet. **179:**547–554.
20. **Kolisnychenko, V., G. Plunkett III, C. D. Herring, T. Feher, J. Posfai, F. R. Blattner, and G. Posfai.** 2002. Engineering a reduced *Escherichia coli* genome. Genome Res. **12:**640–647.
21. **Livingston, D. M., and P. Leder.** 1969. Deformylation and protein biosynthesis. Biochemistry **8:**435–443.

22. **Miller, J. H.** 1972. Experiments in molecular genetics. Cold Spring Harbor Laboratory Press, Cold Spring Harbor, NY.
23. **Nam, K., U. Bläsi, M. T. Zagotta, and R. Young.** 1990. Conservation of a dual-start motif in P22 lysis gene regulation. J. Bacteriol. **172:**204–211.
24. **Park, T., D. K. Struck, J. F. Deaton, and R. Young.** 2006. Topological dynamics of holins in programmed bacterial lysis. Proc. Natl. Acad. Sci. U. S. A. **103:**19713–19718.
25. **Powell, B. S., M. P. Rivas, D. L. Court, Y. Nakamura, and C. L. Turnbough, Jr.** 1994. Rapid confirmation of single copy lambda prophage integration by PCR. Nucleic Acids Res. **22:**5765–5766.
26. **Raab, R., G. Neal, C. Sohaskey, J. Smith, and R. Young.** 1988. Dominance in lambda *S* mutations and evidence for translational control. J. Mol. Biol. **199:**95–105.
27. **Rajagopalan, P. T., S. Grimme, and D. Pei.** 2000. Characterization of cobalt (II)-substituted peptide deformylase: function of the metal ion and the catalytic residue Glu-133. Biochemistry **39:**779–790.
28. **Ramanculov, E. R., and R. Young.** 2001. An ancient player unmasked: T4 rI encodes a t-specific antiholin. Mol. Microbiol. **41:**575–583.
29. **Smith, D. L., C. Y. Chang, and R. Young.** 1998. The λ holin accumulates beyond the lethal triggering concentration under hyper-expression conditions. Gene Expr. **7:**39–52.
30. **Smith, D. L., D. K. Struck, J. M. Scholtz, and R. Young.** 1998. Purification and biochemical characterization of the lambda holin. J. Bacteriol. **180:**2531–2540.
31. **Steiner, M., and U. Bläsi.** 1993. Charged amino-terminal amino acids affect the lethal capacity of lambda lysis proteins S107 and S105. Mol. Microbiol. **8:**525–533.
32. **Takeda, M., and R. E. Webster.** 1968. Protein chain initiation and deformylation in B. subtilis homogenates. Proc. Natl. Acad. Sci. U. S. A. **60:**1487–1494.
33. **Tran, T. A., D. K. Struck, and R. Young.** 2007. The T4 RI antiholin has an N-terminal signal anchor release domain that targets it for degradation by DegP. J. Bacteriol. **189:**7618–7625.
34. **Tran, T. A. T., D. K. Struck, and R. Young.** 2005. Periplasmic domains define holin-antiholin interactions in T4 lysis inhibition. J. Bacteriol. **187:**6631–6640.
35. **von Heijne, G.** 1989. Control of topology and mode of assembly of a polytopic membrane protein by positively charged residues. Nature **341:**456–458.
36. **Vukov, N., I. Moll, U. Bläsi, S. Scherer, and M. J. Loessner.** 2003. Functional regulation of the Listeria monocytogenes bacteriophage A118 holin by an intragenic inhibitor lacking the first transmembrane domain. Mol. Microbiol. **48:**173–186.
37. **Wang, I. N., D. L. Smith, and R. Young.** 2000. Holins: the protein clocks of bacteriophage infections. Annu. Rev. Microbiol. **54:**799–825.
38. **Young, R.** 2002. Bacteriophage holins: deadly diversity. J. Mol. Microbiol. Biotechnol. **4:**21–36.
39. **Young, R., I. N. Wang, and W. D. Roof.** 2000. Phages will out: strategies of host cell lysis. Trends Microbiol. **8:**120–128.
40. **Zagotta, M. T., and D. B. Wilson.** 1990. Oligomerization of the bacteriophage lambda S protein in the inner membrane of Escherichia coli. J. Bacteriol. **172:**912–921.